Journal of Organometallic Chemistry, 439 (1992) 177–188
Elsevier Sequoia S.A., Lausanne
JOM 22857

Structural aspects of the osmium and ruthenium clusters $[M_3(CO)_{10}(alkyne)]$ and related substituted compounds

Antony J. Deeming and Andrew M. Senior
Department of Chemistry, University College London, 20 Gordon Street, London WC1H 0AJ (UK)

(Received April 3, 1992)

Abstract

The synthesis and single-crystal structure determination of the cluster $[Os_3(CO)_{10}(\mu_3\text{-}MeO_2CC_2CO_2Me)]$, derived from the bis-acetonitrile complex $[Os_3(CO)_{10}(MeCN)_2]$ and the alkyne $MeO_2CC{\equiv}CCO_2Me$, are described. The alkyne C–C bond is approximately parallel to an Os–Os edge and one CO ligand is bridging. Distinct distortions from an idealized structure with C_s symmetry are apparent, as previously noted for this class of compound, and a comparison with nine other reported structures of related osmium and ruthenium clusters is presented. Essentially all situations are encountered between two extremes: a structure close to C_s symmetry with a symmetrical μ-CO and a parallel alkyne and another with only terminal CO and a rather more distorted alkyne coordination. There is a clear correlation between the geometry of the bridging CO, metal–metal distances, and the arrangement of the μ_3-alkyne. IR spectra indicate that there are different structures in solution in some cases.

Introduction

There are now several reported crystal structures for the osmium and ruthenium compounds of the type $[M_3(CO)_{10}(alkyne)]$ (M = Ru or Os) and for tertiary phosphine substituted derivatives of these [1–6]. Two broadly different structural types are apparent (**1** and **2** in Fig. 1) and the fluxionality of the system relates partially to the accessibility of these different forms, although the observed rapid alkyne rotation and flipping with respect to the M_3 triangle does not obviously follow from this particular reorganization of the CO shell. Various discussions of the fluxional mechanisms have appeared [e.g., the recent publications, 2, 4]. In this paper we present a new member of the series $[Os_3(CO)_{10}(alkyne)]$ where the alkyne is $MeO_2CC{\equiv}CCO_2Me$ and its crystal structure is described. We have compared the structures of 10 related compounds:

(A) $[Os_3(CO)_{10}(PhC_2Ph)]$ [1];
(B) $[Os_3(CO)_{10}(EtC_2Et)]$ [2];
(C) $[Os_3(CO)_9(EtC_2Et)(PPh_3)]$ [2];

Correspondence to: Professor A.J. Deeming.

0022-328X/92/$05.00 © 1992 – Elsevier Sequoia S.A. All rights reserved

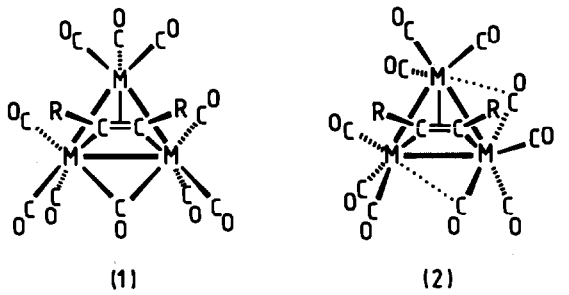

(1) (2)

Fig. 1. Two extreme alkyne structures typified by $[Os_3(CO)_{10}(EtC_2Et)]$ which has approximately the symmetrical structure **1** and $[Os_3(CO)_{10}(PhC_2Ph)]$ which has structure **2**.

(D) $[Os_3(CO)_{10}(HC_2R)]$ [R = $(CO_2)Os_3H(CO)_{10}$] [3];
(E) $[Ru_3(CO)_{10}(HC_2R)]$ [R = $(CO_2)Os_3H(CO)_{10}$] [3];
(F) $[Os_3(CO)_{10}$ $(MeO_2CC_2CO_2Me)]$ [this paper];
(G) $[Os_3(CO)_{10}$ $(HC_2Fc)]$ (Fc = ferrocenyl) [4];
(H) and (I) $[Ru_3(CO)_{10}(MeC_2Me)]$ (two somewhat different geometric forms within the same unit cell) [5];
(J) $[Ru_3(CO)_8(MeO_2CC_2CO_2Me)$ $(PMe_2Ph)_2]$ [6].

We have attempted to see how the unsymmetrical nature of the CO-bridge in form **1** might relate directly to the metal–metal distances and to the twist of the alkyne out of a strictly parallel geometry. Two basic geometries have been found for M_3(alkyne) clusters, with the C–C axis parallel or perpendicular to a M–M direction, respectively, and this paper deals exclusively with the parallel geometry and geometries related to this but with varying degrees of rotation out of this idealized form.

Results and discussion

Synthesis and structure of $[Os_3(CO)_{10}(MeO_2CC_2CO_2Me)]$

This cluster was prepared in low yield (8%) by the room temperature reaction of the alkyne $MeO_2CC{\equiv}CCO_2Me$ with the cluster $[Os_3(CO)_{10}(MeCN)_2]$ and was isolated by TLC on silica. The IR spectrum both in the solid and in solution gave broad ν(CO) absorptions characteristic of a structure with a bridging CO ligand [ν(CO) 1861 cm^{-1} in cyclohexane solution and 1846 cm^{-1} in nujol] unlike $[Os_3(CO)_{10}(PhC_2Ph)]$ which only contains two weakly semi-bridging CO ligands [no solid-state ν(CO) absorptions below 1964 cm^{-1}]. It is related instead to $[Os_3(CO)_{10}(EtC_2Et)]$ which has a fully fledged bridging CO [ν(CO) 1845 cm^{-1} in cyclohexane] [2].

In view of the different structures of the PhC_2Ph [1] and EtC_2Et [2] complexes, we determined the single-crystal X-ray structure of the $MeO_2CC{\equiv}CCO_2Me$ cluster and its molecular structure is shown in Fig. 2. Selected bond lengths and angles are given in Tables 1 and 2. As concluded from the IR data, the overall structure is much more like that of the EtC_2Et than the PhC_2Ph cluster. The alkyne C–C bond, C(2)–C(3), is approximately parallel to the metal edge, Os(1)–Os(2), and there is a bridging CO ligand, C(1b)O(1b). There is a crystallographic problem with disorder of the methoxy groups. The group O(2)C(5) was best refined with the

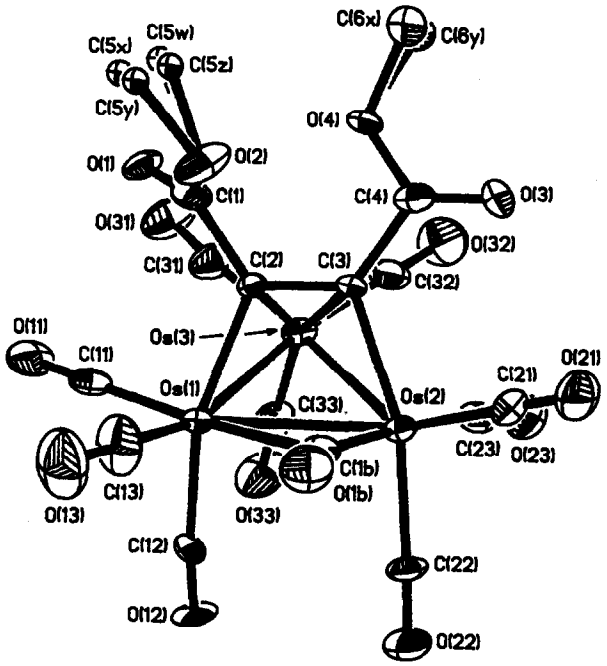

Fig. 2. Molecular structure of the cluster $[Os_3(CO)_{10}(MeO_2CC_2CO_2Me)]$. The methoxy groups are disordered with atoms C(5x) to C(5z) having populations of 0.25 and atoms C(6x) and C(6y) having populations of 0.5.

atom C(5) having 0.25 population in the four different sites shown in Fig. 2. The elongated thermal ellipsoid for O(2) likely indicates that there are also two or more closely positioned sites for this atom corresponding to the different methyl positions, however, a single O(2) position was refined with the populations of the different positions being accommodated within the determined thermal ellipsoid. Likewise the methoxy group O(4)C(6) is disordered and a model with two equally

Table 1

Selected bond lengths (Å) for the cluster $[Os_3(CO)_{10}(MeO_2CC_2CO_2Me)]$

Os(1)–Os(2)	2.850(1)	Os(2)–C(22)	1.98(2)
Os(2)–Os(3)	2.802(1)	Os(2)–C(23)	1.92(3)
Os(1)–Os(3)	2.722(1)	Os(3)–C(31)	1.90(2)
Os(1)–C(2)	2.07(2)	Os(3)–C(32)	1.87(2)
Os(3)–C(2)	2.25(2)	Os(3)–C(33)	1.91(3)
Os(2)–C(3)	2.13(2)	C(1)–C(2)	1.53(2)
Os(3)–C(3)	2.18(2)	C(2)–C(3)	1.40(2)
Os(1)–C(1b)	2.45(2)	C(3)–C(4)	1.51(2)
Os(2)–C(1b)	2.02(2)	C(1)–O(1)	1.14(2)
Os(1)–C(11)	1.90(2)	C(1)–O(2)	1.32(3)
Os(1)–C(12)	1.95(2)	C(4)–O(3)	1.17(2)
Os(1)–C(13)	1.91(2)	C(4)–O(4)	1.30(2)
Os(2)–C(21)	1.90(2)		

Table 2

Selected bond angles (deg) for the cluster $[Os_3(CO)_{10}(MeO_2CC_2CO_2Me)]$

Os(2)–Os(1)–Os(3)	60.3(1)	Os(2)–Os(3)–C(3)	48.6(4)
Os(1)–Os(2)–Os(3)	57.6(1)	Os(1)–C(2)–Os(3)	78.1(6)
Os(1)–Os(3)–Os(2)	62.1(1)	Os(2)–C(3)–Os(3)	81.3(5)
Os(1)–Os(2)–C(1b)	57.3(6)	Os(1)–C(2)–C(3)	112(1)
Os(2)–Os(1)–C(1b)	44.0(5)	Os(2)–C(3)–C(2)	108(1)
Os(1)–C(1b)–Os(2)	78.6(8)	Os(3)–C(2)–C(3)	69(1)
Os(1)–C(1b)–O(1b)	127(2)	Os(3)–C(3)–C(2)	75(1)
Os(2)–C(1b)–O(1b)	155(2)	C(2)–Os(3)–C(3)	36.8(5)
Os(1)–Os(2)–C(3)	69.4(4)	C(1)–C(2)–C(3)	124(1)
Os(2)–Os(1)–C(2)	69.9(4)	C(2)–C(3)–C(4)	125(1)
Os(1)–Os(3)–C(2)	48.0(4)		

populated methyl positions was refined; the thermal ellipsoid for O(4) is elongated as for O(2). This disorder in the alkyne substituents does not appear to have any great consequencies for the geometry of attachment of the alkyne to the Os atoms. The bridging CO is not symmetrical [Os(1)–C(1b) 2.45(2) and Os(2)–C(1b) 2.02(2) Å] and adopts an intermediate geometry between that of the PhC_2Ph ligand [Os–C 2.765(10) and 1.944(12) Å] and the EtC_2Et ligand [Os–C 2.302(18) and 2.086(20) Å] in the corresponding complexes. The structure is closer to that of the EtC_2Et compound but is approximately 30% away from this towards that of the PhC_2Ph compound. The shift of the bridging CO ligand from a totally central position and other features of the structure are discussed comparatively in the next section.

A structural comparison of the clusters $[M_3(CO)_{10}(alkyne)]$ (M = Ru or Os) and related tertiary phosphine-substituted derivatives

As indicated in the introduction, 10 structures of this type have been determined, A–J, and here we compare these results. Figure 3 is a plot of the two M–C bond lengths, *a* and *b*, associated with the bridging CO ligands in these structures. The top left-hand part of the curve corresponds to a symmetrical situation ($a = b$) and closest to this is the more symmetrical of the two molecules of $[Ru_3(CO)_{10}(MeC_2Me)]$ (two rather different structures are found in the unit cell) [$a = 2.167(5)$ and $b = 2.120(5)$ Å]. The biggest difference between *a* and *b* is found for $[Os_3(CO)_9(PPh_3)(EtC_2Et)]$ [$a = 2.920(11)$ and $b = 1.945(11)$ Å]. Figure 4 shows the relation between the angles at the bridging CO and the distances of the carbon atom to the metal atoms, both expressed as ratios. As the CO ligand moves from bridging to terminal, or rather to a very weakly semi-bridging situation, the short M–C bond becomes even shorter as expected, since terminal M–C bonds are shorter than bridging ones. For example, the average terminal M–C distance in the new structure reported in this paper is 1.92 Å compared with 2.45(2) and 2.02(2) Å for the M–C distances in the CO bridge. The displacement of a symmetrical bridging CO ligand, via various unsymmetrical positions, through to an essentially terminal site comes to a stop when a second semi-bridging CO contact develops along another M–M bond (see Fig. 1). The limit seems to be when the two long M–C distances for the semi-bridging CO ligands are roughly equal (2.77 and 2.75 Å in the PhC_2Ph complex).

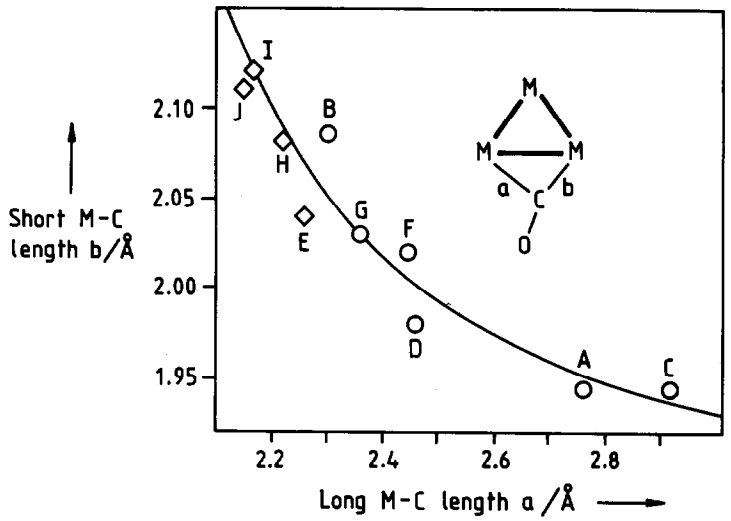

Fig. 3. Plot of the long *versus* the short M–C bond lengths associated with the bridging CO ligands in clusters of the type $[M_3(CO)_{10}(alkyne)]$ and substituted forms (◇, Ru; ○, Os).

A key feature observed in this, as in many other similar analyses, is that all structural situations between the two extremities are encountered; Figs. 3 and 4 show a fairly even scatter of points along each of the curves. When a tertiary phosphine has been introduced as in $[Os_3(CO)_9(PPh_3(EtC_2Et)]$, the CO bridge has the choice of moving towards a terminal site on a PPh_3-substituted metal or on an unsubstituted one. In this case, the move is towards the PPh_3-substituted osmium atom even though one might have imagined that this might produce unfavourable crowding at this atom. The substituted metal atom is the better π-donor and this is likely to be an important factor in favouring the accummulation of terminal CO

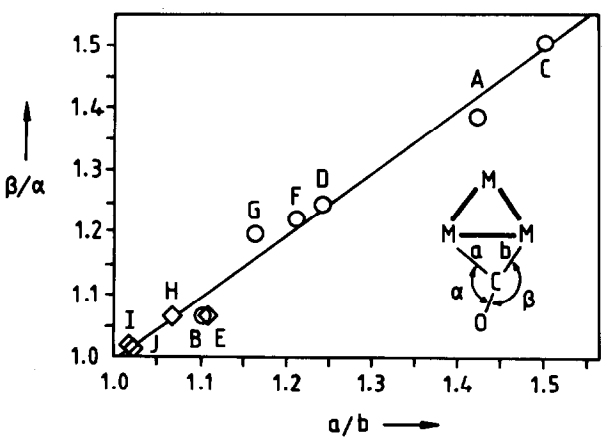

Fig. 4. Plot of the angle ratio β/α *versus* the length ratio a/b for the bridging carbonyl ligands in clusters of the type $[M_3(CO)_{10}(alkyne)]$ and substituted forms (◇, Ru; ○, Os).

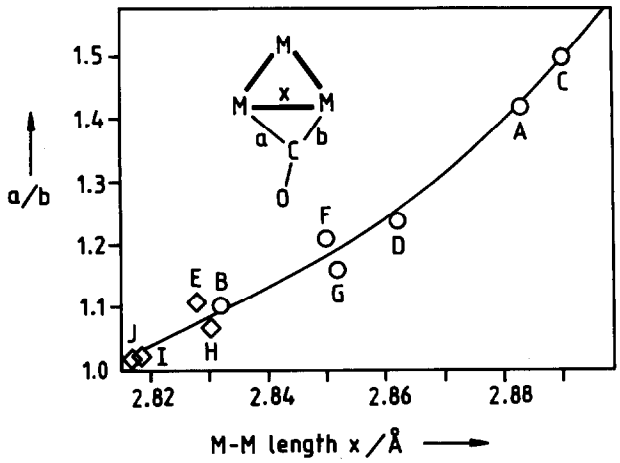

Fig. 5. Plot of the ratio of the M–C bond lengths for the bridging CO (a/b) *versus* the M–M distance (x) which the CO ligand spans in clusters of the type $[M_3(CO)_{10}(alkyne)]$ and substituted forms (◇, Ru; ○, Os).

ligands at this atom. The conversion of structure **1** to **2** (Fig. 1) also requires a small turnstile rotation of each $M(CO)_3$ group.

It is a commonly used argument that bridging CO ligands are more easily accommodated along shorter metal–metal bonded edges. For example, the increase in metal–metal bond lengths on going down a group from first to third row transition metal carbonyls has been used to explain the frequently observed changes of structure from bridged to non-bridged forms. In this series of compounds, there is a very strong correlation between the mode of bonding of the CO and the metal–metal distance. Figure 5 is a plot of the M–CO bond length ratio a/b (a measure of how symmetrical the bridging CO is) against the length of the bridged metal–metal bond. The symmetrically bridging CO ligand is associated with the shorter M–M bond and the four known Ru structures (marked ◇) are found at the bottom end of the curve as expected. However the range of Os–Os bond distances observed, 2.832(1)–2.890(1) Å, is sufficient for an almost complete range of structural types to be adopted in the triosmium systems. It is commonly argued that carbonyl ligands bridge symmetrically, unsymmetrically or terminally because the metal–metal bonds are of a particular length. One might also argue that particular electronic requirements necessitate a particular mode of CO coordination and because of this, the metal–metal distance is what it is. For example, if a symmetrical CO bridge is favoured, then the M–M distance must be short. It is likely that both variables plotted in Fig. 5 have a common origin. Tertiary phosphine substitution has been shown in particular cases to lead to an increase in M–M bond length and this was used to explain a change of structure from the bridged form, $[Os_3(CO)_{10}(EtC_2Et)]$, to the non-bridged (weakly semi-bridged) form of $[Os_3(CO)_9(PPh_3)(EtC_2Et)]$ [2]. However, the M–M bond length in the disubstituted cluster $[Ru_3(CO)_8(PMe_2Ph)_2(MeO_2CC_2CO_2Me)]$ [2.817(1) Å] is no longer than in decacarbonyl compounds of type $[Ru_3(CO)_{10}(alkyne)]$; 2.8304(7), 2.8186(7) and 2.828(4) Å for the corresponding Ru–Ru distance in the ruthenium compounds plotted in Fig. 5. Nor can it be this particular alkyne

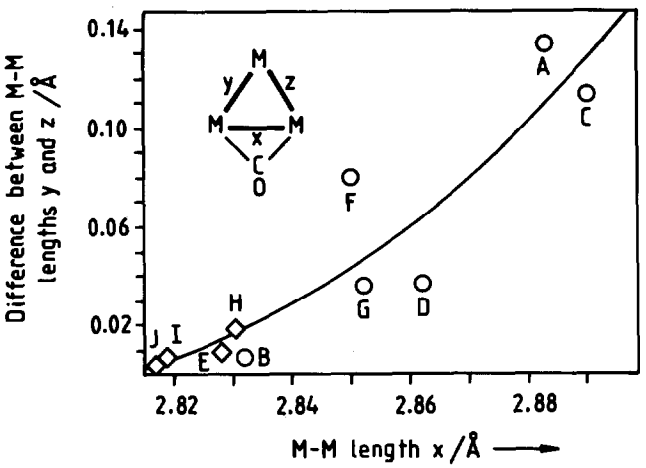

Fig. 6. Relation between M–M bond lengths. Plot of the difference between the bond lengths y and z *versus* the lengths x associated with the CO bridge for clusters of the type $[M_3(CO)_{10}(alkyne)]$ and substituted forms (◇, Ru; ○, Os).

($MeO_2CC_2CO_2Me$) that leads to a metal–metal bond shortening in the disubstituted Ru_3 compound because the corresponding Os–Os lengths are 2.883(1), 2.832(1) and 2.850(1) for the PhC_2Ph, EtC_2Et and $MeO_2CC_2CO_2Me$ osmium complexes, respectively, the dicarboxylate ligand leading to a value intermediate between the others. Consequently there seem to be no simple arguments based on the nature of the alkyne or the degree of phosphine substitution to explain the trends observed in Figs. 3–5. There are very small energy differences between the different geometries (see below) and it is not easy therefore to account for the geometries adopted in particular cases. However, we do not believe that the metal–metal distance controls the geometry but rather this is just one of the variables associated with the changes in geometry.

We now consider the distortions within the rest of the molecule that might be associated with the loss of mirror symmetry on going from structure **1** to **2** (Fig. 1). Figure 6 shows that structures closest to **1** (those with short M–M length x) have very similar M–M lengths y and z and that as the M–M distance x increases (with an associated increase in ratio a/b), the difference between lengths y and z also increases. This correlation is not as strong as in the previous plots. A correlation with similar validity is between a parameter we call the horizontal twist and the ratio a/b (Fig. 7). The alkyne could distort out of the strictly parallel arrangement in two ways: horizontally or vertically with respect to the M_3 plane (see Fig. 8). As a measure of these distortions, we have defined horizontal twist as $(d+f)-(c+e)$ and the vertical twist as $(c+d)-(e+f)$, where c–f are the M–C lengths to the alkyne. These are easy to derive from crystallographic data but have quite large errors associated with them. It is clear that there is a reasonably good correlation between the unsymmetrical character of the carbonyl bridge, the bridged metal–metal distance x, the difference between the other two metal–metal bond lengths y and z, and the horizontal twist of the alkyne. On the other hand, the vertical twist of the alkyne is not correlated with any of these (Fig. 9). We conclude that there is very little vertical twist at all for any of the distributed alkynes that have

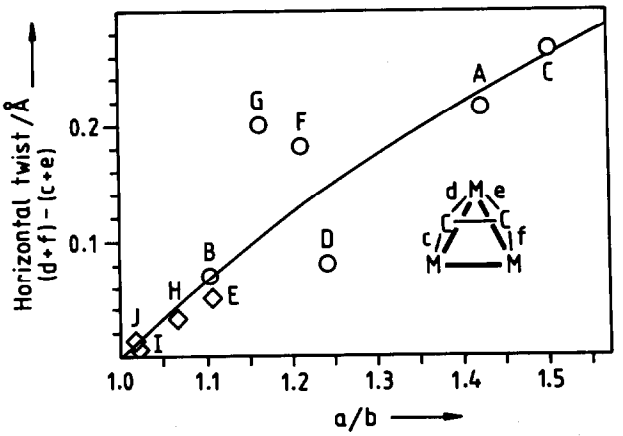

Fig. 7. Plot of the horizontal twist of the alkyne (as defined in terms of the M–C bond lengths $c-f$) in clusters related to $[M_3(CO)_{10}(alkyne)]$ *versus* the ratio a/b as given in earlier figures (◇, Ru; ○, Os).

been studied (shown as open points in Fig. 9), but there is an observable vertical twist for the three mono-substituted alkynes that have been studied so far (closed points in Fig. 9). The CH group makes a significantly closer approach to the metal atoms than do the CR groups.

Some comments on the fluxionality of these clusters

Several authors have reported on the ability of parallel but not perpendicular alkynes to undergo facile horizontal rotation with respect to the metal triangle, this process involving a rotation coupled with a flip so that the opposite faces of the disubstituted alkyne are successively presented to a metal atom in the dihapto coordination as the alkyne rotates with respect to the M_3 triangle. This flip, for example, is apparent from the coalescence of diastereotopic CH_2 proton signals in the NMR spectrum of $[Os_3(CO)_{10}(EtC_2Et)]$ [2]. Hardcastle *et al.* [4] and Rosenberg *et al.* [2] have discussed the mechanism for the decacarbonyl complexes of the type in this paper. In a detailed study, Rosenberg *et al.* identified two processes

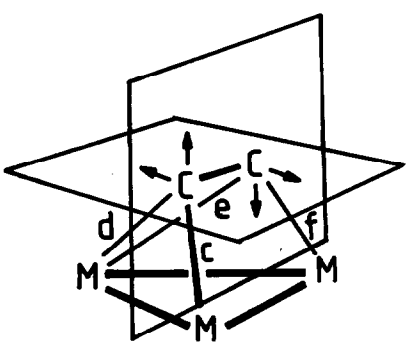

Fig. 8. Representation of horizontal and vertical twists of alkynes in trimetallic clusters, M_3(alkyne). For simplicity we have defined these twists in terms of the M–C(alkyne) distances, c, d, e and f. Horizontal twist $=(d+f)-(c+e)$ and vertical twist $=(c+d)-(e+f)$.

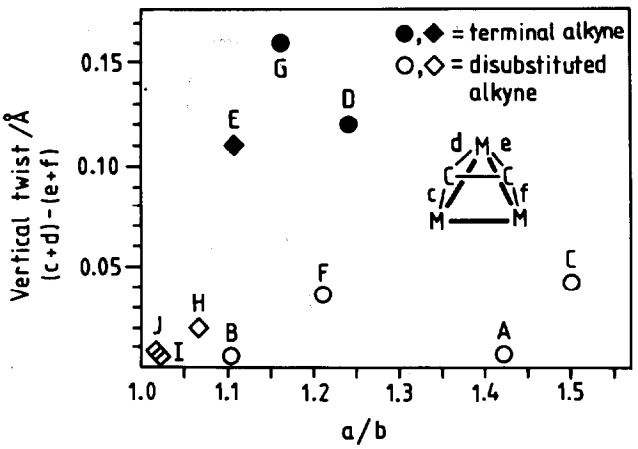

Fig. 9. Plot of the vertical twist of the alkyne in clusters related to $[M_3(CO)_{10}(alkyne)]$ (as defined in terms of the M–C bond lengths $c-f$) *versus* the ratio a/b as given in earlier figures (◇, Ru; ○, Os).

for $[Os_3(CO)_{10}(RC_2R)]$: a localized axial–radial exchange of the terminal CO ligands at the equivalent Os atoms of **1** as the fastest process, while exchange of the bridging CO with the six terminal CO at the bridged metal atoms is rather slower. This latter process is the one that leads to alkyne motion over the face of the metal triangle so we assume that a movement of CO from bridge to terminal sites is linked to alkyne rotation. Even at the lowest temperatures examined, spectra appear to be only consistent with structure **1**, which means that the interconversion between **1** and **2** must be rapid to give a time-averaged mirror plane at the lowest temperatures [2]. The ^{13}C NMR shifts for the bridging CO ligands vary considerably from compound to compound and with temperature [2]. This may be interpreted as resulting from different equilibrium ratios of **1**, **2**, and possibly intermediate structures, and a significant temperature dependence of the equilibrium coefficient(s). Even when the solid-state form has the non-CO-bridged form **2**, as is the case for $[Os_3(PhC_2Ph)(CO)_{10}]$ (IR and XRD data), weak bridging CO absorptions are observed for solution spectra. For example, Fig. 10 shows solid-state and solution spectra for representative compounds with solid-state forms close to structures **1** and **2**, respectively. The solid-state spectra correspond closely to the crystal structures, of course. The $MeO_2CC_2CO_2Me$ compound maintains its solid-state structure in solution and this is essentially true for the PhC_2Ph compound, except that there is a very weak absorption at 1854 cm^{-1} not present in the solid state. The spectrum of a very concentrated solution of $[Os_3(PhC_2Ph)(CO)_{10}]$ (Fig. 11) shows this absorption very clearly. This spectrum is interpreted in terms of structure **2** in equilibrium with a low concentration of **1**. To explore possible electronic effects that might shift this equilibrium, we synthesized the diarylalkyne clusters $[Os_3(ArC_2Ar)(CO)_{10}]$, where Ar = 4-MeC_6H_4, 4-$MeOC_6H_4$ and C_6H_5, and found that their solid-state and solution spectra are essentially indistinguishable in the carbonyl region. Each shows weak bridging CO absorptions in solution: ν(CO) 1855 (Ar = 4-MeC_6H_4), 1855 (Ar = 4-$MeOC_6H_4$) compared with 1854 (Ar = C_6H_5) cm^{-1}. However, replacement of just one aryl by an alkyl group switched the equilibrium over to structure **1**. Thus $[Os_3(PhC_2Me)$-

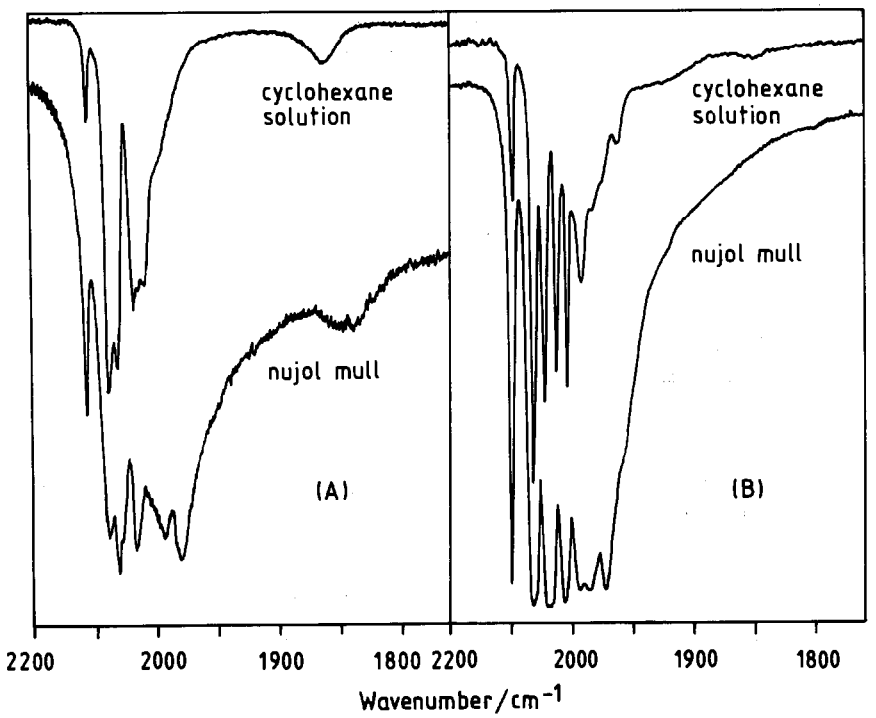

Fig. 10. IR spectra in the CO stretching region for clusters $[M_3(CO)_{10}(alkyne)]$, where alkyne = PhC_2Ph (B) or $MeO_2CC_2CO_2Me$ (A), in the solid state (nujol mulls) and in cyclohexane solution.

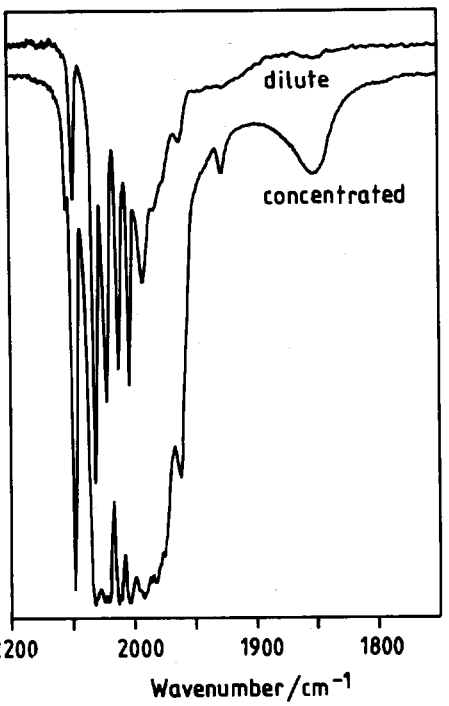

Fig. 11. IR spectra of cyclohexane solutions of $[Os_3(CO)_{10}(PhC_2Ph)]$ at two different concentrations indicating the presence of a bridging CO species in low concentrations.

$(CO)_{10}$] has solid-state and solution IR spectra very similar to those for Os_3-$(MeO_2CC_2C_2Me)(CO)_{10}$] shown in Fig. 10.

Experimental

Syntheses

Compounds of the type $[Os_3(alkyne)(CO)_{10}]$ were synthesized by standard methods from $[Os_3(CO)_{10}(MeCN)_2]$ and the alkyne in dichloromethane at room temperature, followed by chromatographic separation on silica (TLC). Yields varied from moderate to poor: PhC_2Ph (36%), $(4\text{-}MeC_6H_4)_2C_2$ (35%), $(4\text{-}MeOC_6H_4)_2C_2$ (60%), $MeO_2CC_2CO_2Me$ (8%) and PhC_2Me (54%).

Table 3

Fractional atomic coordinates ($\times 10^4$) for the cluster $[Os_3(CO)_{10}(MeO_2CC_2CO_2Me)]$

	x	*y*	*z*
Os(1)	8161(1)	1457(1)	6075(1)
Os(2)	7596(1)	1687(1)	4144(1)
Os(3)	6374(1)	2637(1)	5463(1)
C(1)	8461(14)	4135(15)	6368(13)
C(2)	8092(14)	3162(13)	5714(10)
C(3)	7710(14)	3315(12)	4790(11)
C(4)	7602(15)	4455(15)	4304(13)
C(5W)	9588(51)	5588(62)	6557(65)
C(5X)	9795(70)	5381(62)	6879(46)
C(5Y)	10139(50)	5271(56)	6694(61)
C(5Z)	9881(70)	5509(67)	6419(49)
C(6X)	7859(37)	6451(36)	4553(27)
C(6Y)	7307(32)	6442(32)	4518(24)
O(1)	8052(11)	4434(10)	6992(8)
O(2)	9378(12)	4485(13)	6105(11)
O(3)	7486(14)	4567(12)	3502(9)
O(4)	7620(17)	5290(10)	4889(9)
C(1B)	9108(18)	1406(17)	4684(14)
O(1B)	9987(13)	1281(14)	4653(11)
C(11)	7823(15)	1695(14)	7303(15)
O(11)	7655(15)	1868(13)	8011(10)
C(12)	7716(25)	−139(16)	6070(12)
O(12)	7389(21)	−996(11)	5993(10)
C(13)	9615(19)	1166(27)	6486(17)
O(13)	10443(16)	966(21)	6815(13)
C(21)	8218(19)	2158(18)	3066(13)
O(21)	8682(14)	2430(15)	2446(10)
C(22)	7469(17)	27(15)	3909(13)
O(22)	7404(15)	−900(12)	3813(11)
C(23)	6196(22)	1867(16)	3532(16)
O(23)	5387(16)	1915(16)	3093(12)
C(31)	6063(21)	3379(20)	6559(16)
O(31)	5763(14)	3874(17)	7160(12)
C(32)	5386(20)	3515(17)	4732(16)
O(32)	4769(17)	4036(19)	4281(15)
C(33)	5508(19)	1374(21)	5756(16)
O(33)	4982(16)	607(17)	5901(14)

Single crystal structure determination for $[Os_3(CO)_{10}(MeO_2CC_2CO_2Me)]$

An irregularly shaped chip of a large single crystal of the compound $C_{16}H_6O_{14}Os_3$, $M = 992.82$, $0.3 \times 0.4 \times 0.4$ mm^3, was mounted on a Nicolet R3v/m diffractometer. A monoclinic cell, $a = 12.608(3)$, $b = 11.725(4)$, $c = 14.570(4)$ Å, $\beta = 95.31(2)°$, $U = 2145(1)$ Å^3 was determined by auto-indexing and least-squares refinement of 30 orientation reflections in the range $9 \leq 2\theta \leq 26°$; 4949 unique intensity data were collected at 17°C using graphite monochromated Mo-K_α radiation ($\lambda = 0.71073$ Å) in the ω–2θ scan mode between $5 \leq 2\theta \leq 55°$. The intensities were corrected for Lorentz and polarization effects, for a small decay during the collection based on the intensities of three standard reflections, and empirically for absorption; μ(Mo-K_α) = 178.3 cm^{-1}.

The structure was solved by direct methods in the space group $P2_1/n$, $Z = 4$, $F(000) = 1768$, $D_c = 3.07$ g cm^{-3}. A model with 301 parameters was refined to $R = 0.0653$, $R_w = 0.0605$ using 3690 intensity data with $F_o \geq 3\sigma(F_o)$. All non-H atoms were refined anisotropically except for the methoxy carbon atoms which were disordered. H-atoms were not included. The best model to account for the disorder gave two positions for C(6) with 0.5 occupancy each and four positions for C(5) with occupancy of 0.25. Thermal parameters for these four partial carbon atoms were fixed as equal but refined. The thermal parameters for the oxygen atoms to which C(5) and C(6) were attached, suggested a small degree of disorder for these atoms but this was not modelled. The structure of the CO_2Me substituents remains poorly defined. The largest peak in the difference Fourier map was 3.8 e Å^{-3} close to an osmium atom and the largest shift-to-e.s.d. ratio in the final least-squares cycle was 0.004 except for the disordered Me carbons for which the maximum shift was 0.04. Atomic coordinates for the cluster are given in Table 3. A complete list of bond lengths and angles and a list of observed and calculated structure factors are available from the authors.

All calculations were carried out using a MicroVax II computer running SHELXTL-PLUS.

Acknowledgment

We thank the SERC for an award towards the purchase of the diffractometer.

References

1 (a) M. Tachikawa, J.R. Shapley and C.G. Pierpont, J. Am. Chem. Soc., 97 (1975) 7172; (b) C.G. Pierpont, Inorg. Chem., 16 (1977) 636.
2 E. Rosenberg, J. Bracker-Novak, R.W. Gellert, S. Aime, R. Gobetto and D. Osella, J. Organomet. Chem., 365 (1989) 163.
3 K.I. Hardcastle, T. McPhillips, A.J. Arce, Y. De Sanctis, A.J. Deeming and N.I. Powell, J. Organomet. Chem., 389 (1990) 361.
4 K.I. Hardcastle, A.J. Deeming, D. Nuel and A.J. Deeming, J. Organomet. Chem., 375 (1989) 217.
5 S. Rivomanana, G. Lavigne, N. Lugan and J.-I. Bonnett, Organometallics, 10 (1991) 2285.
6 M.I. Bruce, P.A. Humphrey, H. Miyamae and A.H. White, J. Organomet. Chem., 417 (1991) 431.